Journal of Non-Crystalline Solids 499 (2018) 283–288

Contents lists available at ScienceDirect

Journal of Non-Crystalline Solids

journal homepage: www.elsevier.com/locate/jnoncrysol

Acoustic characterization of silica aerogel clamped plates for perfect absorption

A. Geslain[a], J.-P. Groby[b], V. Romero-García[b,*], F. Cervera[c], J. Sánchez-Dehesa[c]

[a] DRIVE EA1859, Univ. Bourgogne Franche Comté, F58000 Nevers, France
[b] Laboratoire d'Acoustique de l'Université du Mans, L'Université Nantes Angers Le Mans, Université du Mans, UMR CNRS 6613, Avenue Olivier Messiaen, 72085 Le Mans, France
[c] Wave Phenomena Group, Departamento de Ingeniería Electrónica, Universitat Politècnica de València, Camino de vera s/n (Edificio 7F), E-46022 València, Spain

ARTICLE INFO

Keyword:
Aerogel
Acoustics
Mechanical characterization
Genetic algorithm.

ABSTRACT

A multiobjective optimization procedure is employed to retrieve the viscoelatic parameters of silica aerogel clamped plates. This retrieval method preserves the aerogel sample integrity and, in contrast to the existing ones, relies on the minimization of two different cost functions. The first one, namely J_1, is related to the reflective properties of clamped plates backed by a rigid cavity, while the second one, namely J_2, concerns both the reflectance and transmittance spectra measured in transmission configuration. The recovered parameters are in agreement with previously reported values in the literature. In addition, they are also supported by designing structures for perfect absorption (100% of absorption), which has been validated experimentally. Aerogel plates can be therefore used as innovative building units of artificial structures for the broadband absorption of sound.

1. Introduction

Silica aerogels have been mainly developed for thermal and acoustic insulation purposes [1;2]. Therefore, their manufacturing process has been widely studied to improve their bulk properties and they present an extremely low density [3], an ultra low thermal conductivity [4], and a subsonic sound velocity [5;6]. The extremely low static density is directly related to their high porosities. The frame of silica aerogel effectively consists of an assembly of connected small cross-sections beam-like elements resulting from fused nanoparticles. This particular assembly additionally provides silica aerogel a very low elastic stiffness when compared to rigid silica structure of identical porosity [6]. Silica aerogels are then nanoporous lightweight materials [2]. Beyond these soft bulk material properties, silica aerogel plates or membranes are excellent candidates to design original acoustic metamaterials, because they exhibit subwavelength resonances and present efficient absorption capabilities [7].

Recently, membrane-type metamaterials have shown an increasing interest to control acoustic waves. While a single membrane presents negative mass density [8] as well as may be used as a perfect subwavelength absorber [9;10], the periodic arrangement of plates combined with other kind of resonators presents single and double negativity [11]. More recently, periodic arrangement of clamped plates has been used to control the harmonic generation [12] and the solitary wave generation in the nonlinear acoustic regime [13].

The characterization of the elastic properties of the silica aerogel plates is therefore primordial to design efficient aerogel-based acoustic metamaterials. Two types of test have been yet proposed to characterize their elastic properties: mechanical destructive tests and ultrasonic non-destructive tests. On the one hand, Woignier et al. [14;15;16] used 3-point bending and uniaxial compression while Haj-Ali et al. [17] used digital image correlation technique to determine the mecanical behavior of aerogel. On the other hand, ultrasonic tests [5;6;18;19] provide acoustic properties but are limited in terms of frequencies and by definition do not provide information in the audible regime.

This work aims at providing the viscoelastic properties of silica aerogel plates in the audible frequency range thanks to a novel signal processing method based on usual impedance tube measurements which have the advantage to preserve the sample integrity. The silica aerogel, being nanoporous, can be approximated by a viscoelastic material in this low frequency regime; i.e. in the audible frequency range. In this work we also show that clamped plates of silica aerogel can be used to design ultralight acoustic metamaterials for the perfect absorption of sound.

The article is divided in four Sections. In Section 2, the proposed method to retrieve the elastic properties is presented. A genetic optimization algorithm is used with two objective (or cost) functions to estimate Young modulus, loss factor, Poisson's ratio and mass density of

* Corresponding author.
E-mail address: virogar1@gmail.com (V. Romero-García).

https://doi.org/10.1016/j.jnoncrysol.2018.07.021
Received 2 May 2018; Received in revised form 5 July 2018; Accepted 9 July 2018
Available online 26 July 2018

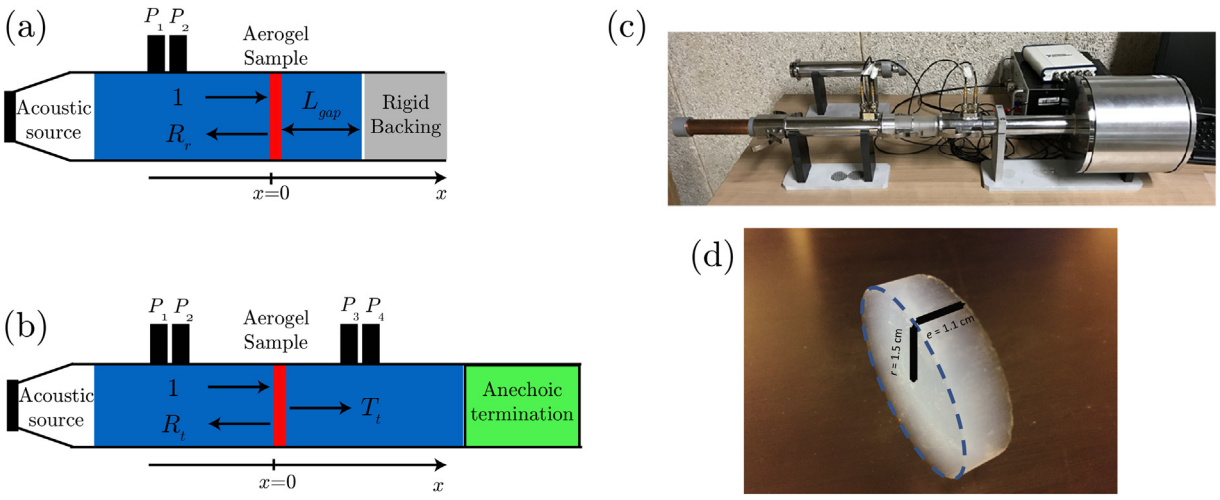

Fig. 1. Reflection and transmission configurations and experimental set-up. (a) acoustic reflection configuration to determine reflection coefficient from the evaluated pressure P_1, P_2. (b) acoustic transmission problem to assess reflection and transmission coefficients from the pressures P_1, P_2, P_3, P_4. (c) Acoustic impedance tube mounted for the experimental characterization of the transmission problem. (d) Photograph of a Silica aerogel plate with thickness $e = 1.1$ cm and radius $r = 1.5$ cm.

the sample. The two objective functions arise from two complementary acoustic configurations: the reflection problem, where the aerogel membrane is backed with a rigid cavity, and the transmission problem. Section 3 make use of the recovered parameters to derive the perfect absorption (PA) condition [9;20] (i.e. $\alpha = 1$, where α is the acoustic absorption) when the silica-aerogel plate is backed by a rigid cavity of a specific length. By varying the cavity length from 0.5 cm to 6.5 cm, the positions of both zeros and poles of the reflection coefficients are studied in the complex frequency domain. Section 4 provides the concluding remarks and comments.

2. Acoustic characterization of the silica aerogel plate mechanical properties

The characterization of the viscoelastic properties of the silica aerogel plate is based on the analysis of data acquired in the two configurations shown in Fig. 1. In the first one, depicted in Fig. 1(a), the reflection coefficient of the aerogel plate when rigidly backed with an air cavity is measured. In the second one, depicted in Fig. 1(b), both the reflection and transmission coefficients of the aerogel plate in a transmission problem are measured. In addition, Fig. 1(c) shows a photograph of the experimental setup used for the characterization.

In this Section, we present the retrieval procedure which consists in minimizing the difference between the experimental and the theoretical coefficients.

2.1. Direct modeling

Assuming a Kirchhoff-Love plate [21], the transverse displacement w_s satisfies the equation of motion

$$D\nabla^4 w_s + e\rho\frac{\partial^2 w_s}{\partial t^2} = 0, \tag{1}$$

where e is the plate thickness, ρ is the plate density and D is the flexural rigidity. $D = \frac{Ee^3}{12(1-\nu^2)}$, where E is the Young modulus and ν is the Poisson coefficient. Considering the temporal convention $e^{i\omega t}$, with ω the angular frequency, the silica aerogel viscoelastic behavior implies a complex Young modulus of the form $E = E_r(1 + i\eta\omega)$, where E_r is the real part of the Young modulus and η is the loss factor. Assuming a subwavelength regime, the silica aerogel disk is considered as a punctual resonant element. The acoustic impedance Z_p of a clamped circular cross-section plate was derived [7] and takes the form,

$$Z_p = \frac{-i\omega\rho e}{S}\frac{I_1(k_p r)J_0(k_p r) + J_1(k_p r)I_0(k_p r)}{I_1(k_p r)J_2(k_p r) - J_1(k_p r)I_2(k_p r)} \tag{2}$$

where $S = \pi r^2$ is the cross-section surface of the plate, J_n and I_n are the regular and modified Bessel functions of the first kind of order $n \in \{0, 1, 2\}$ and $k_p^2 = \omega\sqrt{\rho e/D}$ is the plate wavenumber.

In the impedance tube, the aerogel clamped plate acoustically behaves as a point resonator mounted in series, implying sound velocity continuity and pressure discontinuity. Therefore, the clamped plate can be represented by a matrix M_p when using the transfer matrix method, [22] which reads as

$$[M_p] = \begin{bmatrix} M_{p11} & M_{p12} \\ M_{p21} & M_{p22} \end{bmatrix} = \begin{bmatrix} 1 & Z_p \\ 0 & 1 \end{bmatrix}. \tag{3}$$

The reflection and transmission coefficients for this symmetric and reciprocal transmission problem are then directly obtained from the elements of M_p as [22],

$$T = \frac{2e^{ikL}}{M_{p11} + M_{p12}/Z_t + Z_t M_{p21} + M_{p22}}, \tag{4}$$

$$R = \frac{M_{p11} + M_{p12}/Z_t - Z_t M_{p21} - M_{p22}}{M_{p11} + M_{p12}/Z_t + Z_t M_{p21} + M_{p22}}, \tag{5}$$

where $Z_t = \rho_t c_t / S$ is the impedance of the surrounding medium, i.e. in our case the effective fluid occupying in the impedance tube, S is the characteristic cross-sectional area of the tube, k is the wavenumber in the air and L is the length of the sample, in our case $L = e$. Viscous and thermal losses are effectively accounted for in the tube thanks to the formulae provided by Stinson [23].

The aerogel plate system being symmetric and reciprocal, the modeled coefficients in the transmission problem are given by,

$$T^t_{mod} = \frac{2}{2 + Z_p/Z_t}, \qquad R^t_{mod} = \frac{Z_p/Z_t}{2 + Z_p/Z_t}. \tag{6}$$

In the reflection problem, the system is composed of an aerogel plate in front of a closed cavity. In this case, the transfer matrix method reads as,

$$\begin{bmatrix} P \\ V \end{bmatrix}_{x=0} = [M_p][M_c]\begin{bmatrix} P \\ 0 \end{bmatrix}_{x=L_{gap}}, \tag{7}$$

with the propagation matrix M_c given by

$$[M_c] = \begin{bmatrix} \cos(k_t L_{gap}) & iZ_t \sin(k_t L_{gap}) \\ i\sin(k_t L_{gap})/Z_t & \cos(k_t L_{gap}) \end{bmatrix}, \quad (8)$$

where k_t is the wavenumber in the closed cavity (accounting for viscothermal losses) and L_{gap} is the cavity length. The reflection coefficient is thus,

$$R^r_{mod} = \frac{Z_{syst} - Z_t}{Z_{syst} + Z_t}, \quad (9)$$

where $Z_{syst} = P_{x=0}/V_{x=0}$ is the system impedance.

2.2. Measurements of the reflection and transmission coefficients

The reflection and transmission coefficients in each configuration are measured following the recovery of the scattering matrix elements as explained for example in Ref. (24). In the reflection configuration, the two acoustic pressures, P_1 and P_2, are measured by the two microphones located upstream from the material to extract the frequency dependent experimental reflection coefficient $R_{exp}{}^r(f)$ (where f is the frequency). In the transmission problem, Fig. 1(b), the four acoustic pressures, P_1, P_2, P_3, and P_4, are measured by a pair of microphones located upstream and downstream from the material to obtain the experimental reflection and transmission coefficients $R_{exp}{}^t(f)$ and $T_{exp}{}^t(f)$ assuming the sample is symmetric.

The experimental setup is depicted in Fig. 1(c). The diameter of the impedance tube is $d_t = 3$ cm. The experimental data are acquired with an excitation of 3000 sine functions equally spaced between 20 Hz and 6000 Hz. Four 1/4 in. microphones are flush mounted, connected to a spectral analyser and measure the acoustic pressure. Each measurement is averaged 30 times to obtain the transfert function between the microphones. The aerogel samples are presented in Fig. 1(d).

2.3. Retrieval procedure: multiobjective optimization

Decisions on optimal design in many scientific or engineering areas require a compromise between different objectives (or cost functions). It is therefore natural to look for the best solution to each of these cost functions. However, an improvement in one of the cost function can lead to a deterioration in the other ones if some cost functions are conflicting with the other. The absence of a single optimal solution is effectively a difficulty. Multiobjective optimization problems enable to avoid this issue. The optimal solution consists in a set Θ_p named Pareto set [25]. The main characteristic of this set is that none of these elements are better than the others for some of the objectives. This means that all solutions are optimal in some sense.

In this Section we define the cost functions that are minimized by the multiobjective algorithm to retrieve the viscoelastic parameters of the aerogel plates, as well as the criteria chosen to identify the best solution and analyze the Pareto set. For the optimization problem, our approach is based on the use of evolutionary algorithms, which enable the simultaneous generation of several elements of the Pareto set in parallel and in a single run. Among these evolutionary algorithms, genetic algorithms, which are inspired by biological evolution (crossover, mutation, recombination and selection), are used [26]. The individuals of the genetic algorithm are coded by chromosomes of the form, (ρ, ν, E_r, η). An initial population (a set of possible solutions) evolves by applying genetic operators that combine the characteristics of some of the individuals of the population. At each iteration, the population changes and adapts to converge to the optimal solution Θ_p.

2.3.1. The cost functions

To retrieve the viscoelastic properties of the aerogel plate, two cost functions are defined. The two objective functions J_1 (transmission problem) and J_2 (reflection problem) are composed of the L_2 norms of the differences between the experimental and theoretical acoustic reflection and transmission coefficients over a range of frequencies centered on the resonance frequency system considered,

$$J_1 = \sum_{f=f_1}^{f_2} \|R^t_{exp}(f) - R^t_{mod}(\rho,\nu,E,\eta,f)\|^2 + \sum_{f=f_1}^{f_2} \|T^t_{exp}(f) - T^t_{mod}(\rho,\nu,E,\eta,f)\|^2, \quad (10)$$

$$J_2 = \sum_{f=f_1}^{f_2} \|R^r_{exp}(f) - R^r_{mod}(\rho,\nu,E,\eta,f)\|^2, \quad (11)$$

where $R_{exp}{}^t$, $T_{exp}{}^t$ ($R_{mod}{}^t$, $T_{mod}{}^t$) are the experimental (respectively modeled) reflection and transmission coefficients in the transmission problem, and $R_{exp}{}^r$ ($R_{mod}{}^r$) is the experimental (respectively modeled) reflection coefficient in the reflection problem. In the summations $f_1 = 1124$ Hz and $f_2 = 2324$ Hz. Each experimental coefficients were measured several times to check the measurement repeatability. The mechanical properties of the silica aerogel plate being independent of the length of the backing cavity, we chose without loss of generality and for convenience of our experimental setup, the gap thickness $L_{gap} = 0.5$ cm for the reflection problem (see Fig. 1(a)).

2.3.2. Solutions: Pareto front

Fig. 2(a) shows the Pareto fronts of optimization procedure results. Each open circle in the Pareto front represents a solution with a different set of parameters {ρ, ν, E_r, η}. The position of the solution in the Pareto front provides information on the accuracy of the retrieval procedure by using the two configurations previously described. The range of variation of the cost function J_2 is smaller than that of J_1 (see Fig. 2(a)). Therefore, the parameters are less sensitive to the reflection problem than to the transmission problem. In order to compare their accuracy, three solutions are given in Table 1. These three solution are respectively highlighted in the Fig. 2(a) with blue, red and green circles. Among all the solutions, the point (J_1, J_2) = (1.027, 6.308) [(J_1, J_2) = (3.077, 5.786)] represents the best [wrong] solution for the objective J_1, i.e. for the transmission problem, and the worst [best] solution for the objective J_2, i.e. for the reflection problem. We can clearly see in Fig. 2(b,c) [Fig. 2(f,g)] that the differences between the reflection and transmission coefficients obtained for the transmission [reflection] problem are smaller than the ones obtained for the reflection [transmission] problem for this solution. The corresponding estimated parameters are summarized in the Table 1. The retrieval procedure provides relatively identical values of {ρ, E_r, η} at both points. This means the transmission problem is enough to estimate these three parameters. In order to estimate ν, the multiobjective optimization procedure accounting additionally for the reflection problem should be considered.

In the opposite, the point (J_1, J_2) = (1.719, 5.924) represents the solution with the minimal distance to the origin of coordinates, showing that the differences between the theory and the experiments for both problems are similar (see Fig. 2(d,e)). As a consequence, the criterium to choose the best solution is based on the minimal distance to the origin of coordinates, and this point is chosen as the solution of our problem. The retrieved viscoelastic parameters are given in Table 1 and their values are in agreement with others previously reported in the literature [27;28].

In order to further support the viscoelastic parameters provided by the optimization problem, results of reflection problems with different values of the cavity thickness L_{gap} = [0.5, 1, 6.5] cm are compared to measurements. Results of the absolute value and the phase of the reflection coefficients are respectively shown in Fig. 3(a) and (b). Continuous and dotted lines represent respectively the theoretical values and experimental results respectively. The theoretical predictions and experimental data are in good agreement, giving support to the viscoelastic parameters estimated by the proposed optimization procedure

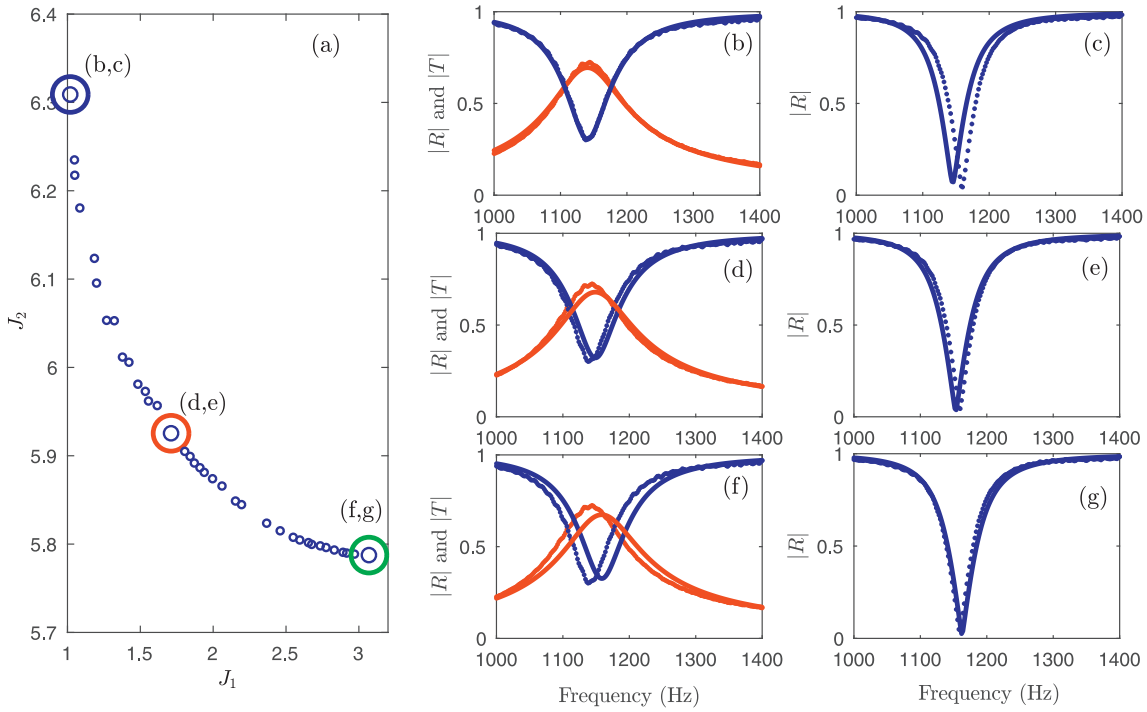

Fig. 2. (a) Pareto front of the two objective functions J_1 and J_2. Big blue (red) [green] circle in (a) represents the Point 1 {2} [3] in Table 1. The reconstructed reflection and transmission coefficients for the transmission problem for this solution are shown in (b) {(d)} [(f)] while the reconstructed reflection coefficient for the reflection problem is shown in (c) {(e)} [(g)]. Full lines represent the theoretical coefficients while dotted lines represents experimental results. (For interpretation of the references to colour in this figure legend, the reader is referred to the web version of this article.)

Table 1
Optimal aerogel mechanical parameters of the three selected points in Fig. 2.

	ρ	ν	E_r	η
	(kg·m^{-3})		(k Pa)	(10^{-6})
Point 1	80	0.09	197.51	4.19
Point 2	80	0.12	197.92	4.47
Point 3	80	0.17	197.99	4.50

and also validating both the measurement and the model approach.

3. Critical coupling condition and perfect absorption

The absorption properties of a system composed of the silica aerogel plate is studied making use of the previously estimated viscoelastic properties. The aerogel plate behaves as a viscoelastic clamped plate with intrinsic losses. The combination of an elastic plate with a back closed cavity, as shown in Fig. 1(a), can be analyzed as an open lossy resonator. In this case, the resonator presents two types of losses, the energy leakage of the open resonator and the intrinsic losses of the system. Recently, the design of perfect absorbers for acoustic wave has received an increasing interest [10;9;29;20;30]. The perfect absorption (PA) condition (i.e. $\alpha = 1$, where α is the acoustic absorption coefficient) is related to the exact counterbalance between the energy leakage of the system and the dissipated energy by the inherent losses [20], which is known as the critical coupling condition. In this Section we show the efficiency of systems based on silica aerogel plates to perfectly absorb the acoustic energy.

In order to provide insights to the perfect absorption process, the reflection coefficient of an aerogel plate backed by a closed cavity is analyzed in the complex frequency plane for different cavity lengths. The cavity length L_{gap} varies between 0.5 cm and 6.5 cm. In the present problem, the eigenvalue of the scattering matrix reduces to the reflection coefficient. The measured reflection coefficient corresponds to the

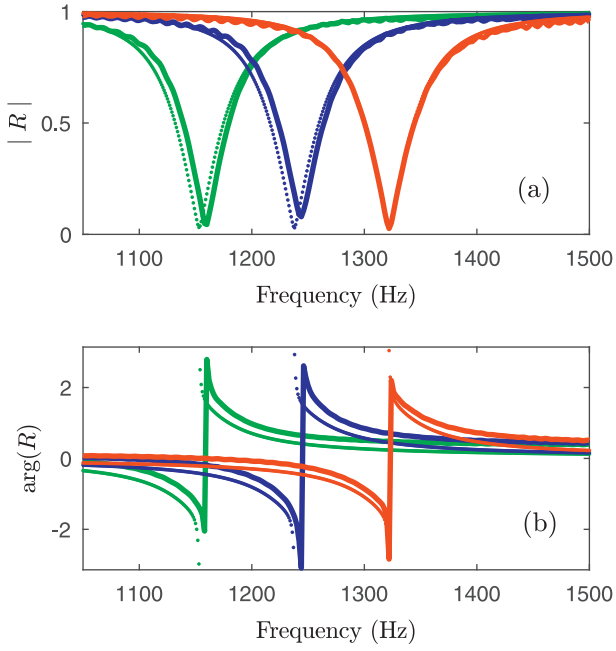

Fig. 3. Comparison of the experimental reflection coefficient (circles) and the reconstructed reflection coefficient (solid lines) [$R_{exp}{}^r$, $R_{mod}{}^r$] for the back cavity length L_{gap} = [0.5, 1, 6.5] cm [red, blue and green lines and symbols respectively]. (For interpretation of the references to colour in this figure legend, the reader is referred to the web version of this article.)

one calculated along the real frequency axis. Therefore, the perfect absorption condition occurs in the complex frequency plane when the zero of the reflection coefficient crosses the real frequency axis [9;20].

Fig. 4(a), (b) and (c) show the reflection coefficient in the complex frequency plane for the configuration with L_{gap} = [0.5, 1, 6.5] cm

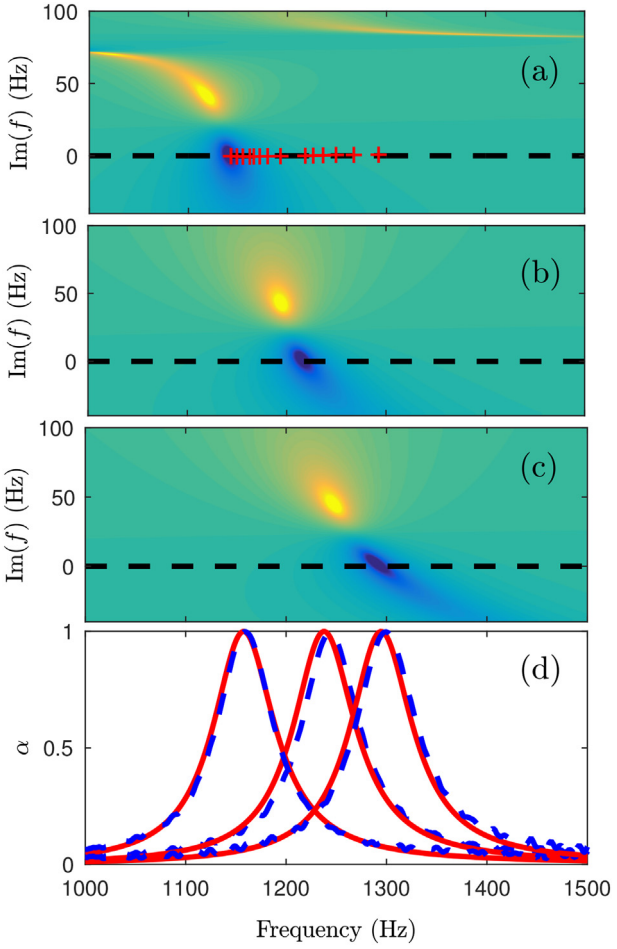

Fig. 4. (a)–(c) Representation of the $log_{10}(|R|^2)$ (colour scale), in the complex frequency plane for the configurations with L_{gap} = {0.5, 1, 6.5} cm respectively. In (a) red crosses represent the complex frequency of the zero of $|R|$ in the complex frequency plane for the configurations L_{gap} = {0.5, 0.6, 0.7, 0.8, 0.9, 1.0, 1.5, 2.0, 2.5, 3.0, 3.5, 4.5, 5.5, 6.5} cm. (d) Comparison of the absorption coefficients, α, for L_{gap} = {0.5, 1, 6.5} cm (in solid line theoretical reconstructed coefficients and in dashed line experimental results). (For interpretation of the references to colour in this figure legend, the reader is referred to the web version of this article.)

respectively. For these three configurations, the zero of the reflection coefficient shifts at low frequencies when cavity length increases and, more importantly, it stands on the real frequency axis. Moreover, the zero of the reflection coefficient of each of these configurations is located exactly on the real frequency axis (red crosses in Fig. 4(a), meaning that all these configurations present perfect absorption. It is remarkable that the frequency at which perfect absorption is obtained is tunable in a broad range of frequencies by tuning L_{gap}.

Perfect absorption was experimentally verified. Red and blue dashed lines in Fig. 4(d) show the theoretical reconstructed predictions and the experimental results respectively. We can see that the frequency at which perfect absorption is obtained corresponds to the situation in which the zero of the reflection coefficients is located on the real frequency axis. The agreement between the theory and the experiments is very good and makes aerogel plate backed by a closed cavity as an innovative artificial structures for acoustic absorption purpose.

4. Summary

A novel signal processing method for retrieving the viscoelastic properties of a silica aerogel clamped plate is presented. This method is based on a genetic algorithm optimization with two objective functions resulting from two acoustic configurations, a reflection problem and a transmission problem in an acoustic impedance tube. The two objective functions are composed of the L_2 norms of the differences between the experimental and modeled acoustic problems around the plate resonance frequency. The estimated aerogel viscoelastic properties are $\rho = 80\,kg/m^3$, $\nu = 0.12$, $E_r = 197.92\,kPa$, $\eta = 4.47\ 10^{-6}$. These values are close to those previously reported in the literature. The main advantages of the present method is that the aerogel silica sample is undamaged and due to the genetic algorithm process the estimated viscoelastic properties satisfy identically the transmission and reflection problems in the audible frequency range. Once the viscoelastic properties of the silica aerogel plate are characterized, the perfect absorption condition (i.e. $\alpha = 1$, with α is the acoustic absorption) is derived for a system consisting in an aerogel plate backed by a rigid cavity. It is shown that such a system possess the ability to perfectly absorb sound over a wide range of cavity length, and therefore over a wide range of possible frequency. The absorptive properties of aerogel are encouraging and can be applied to design more complex artificial structures (metasurfaces) for the broadband absorption of sound.

Acknowledgments

This article is based upon work from COST Action DENORMS CA15125, supported by COST (European Cooperation in Science and Technology). The authors are grateful to the French ANR project Metaudible (ANR-13-BS09-0003) and to RFI Le Mans Acoustique (Région Pays de la Loire) PA*V*Nat and Aerogel projects. F·C and J.S-D. acknowledge the partial support by the Ministerio de Economía y Competitividad of the Spanish Goverment and the European Union "Fondo Europeo de Desarrollo Regional (FEDER)" through project No. TEC2014-53088-C3-1-R.

References

[1] L.W. Hrubesh, Aerogel applications, J. Non-Cryst. Solids 225 (1998) 335.
[2] M. Schmidt, F. Schwertfeger, Applications for silica aerogel products, J. Non-Cryst. Solids 225 (1998) 364–368.
[3] M. Li, H. Jiang, D. Xu, O. Hai, W. Zheng, Low density and hydrophobic silica aerogels dried under ambient pressure using a new co-precursor method, J. Non-Cryst. Solids 452 (2016) 187–193.
[4] Q. Xu, H. Ren, J. Zhu, Y. Bi, Y. Xu, L. Zhang, Facile fabrication of graphite-doped silica aerogels with ultralow thermal conductivity by precise control, J. Non-Cryst. Solids 469 (2017) 14–18.
[5] V. Gibiat, O. Lefeuvre, T. Woignier, J. Pelous, J. Phalippou, Acoustic properties and potential applications of silica aerogels, J. Non-Cryst. Solids 186 (1995) 244–255.
[6] M. Gronauer, J. Fricke, Acoustic properties of microporous SiO2-aerogel, Acta Acust united Ac. 59 (1986) 177.
[7] M. Guild, V.M. García-Chocano, J. Sánchez-Dehesa, T.P. Martin, D.C. Calvo, G.J. Orris, Aerogel as a soft acoustic metamaterial for airborne sound, Phys. Rev. Appl. 5 (034012) (2016).
[8] Z. Yang, J. Mei, M. Yang, N.H. Chan, P. Sheng, Membrane-type acoustic metamaterial with negative dynamic mass, Phys. Rev. Lett. 101 (204301) (2008).
[9] V. Romero-García, G. Theocharis, O. Richoux, A. Merkel, V. Tournat, V. Pagneux, Perfect and broadband acoustic absorption by critically coupled sub-wavelength resonators, Sci. Rep. 6 (19519) (2016).
[10] G. Ma, M. Yang, S. Xiao, Z. Yang, P. Sheng, Acoustic metasurface with hybrid resonances, Nat. Mat. 13 (2014) 873–878.
[11] S.H. Lee, C.M. Park, Y.M. Seo, Z.G. Wang, C.K. Kim, Composite acoustic medium with simultaneously negative density and Modulus, Phys. Rev. Lett. 104 (054301) (2010).
[12] J. Zhang, V. Romero-García, G. Theocharis, O. Richoux, V. Achilleos, D.J. Frantzeskakis, Second-harmonic generation in membrane-type nonlinear acoustic metamaterials, Crystals 6 (2016).
[13] J. Zhang, V. Romero-García, G. Theocharis, O. Richoux, V. Achilleos, D.J. Frantzeskakis, Bright and gap solitons in membrane-type acoustic metamaterials, Phys. Rev. E 96 (2017).
[14] A.H. Alaoui, T. Woignier, G.W. Scherer, J. Phalippou, Comparison between flexural and uniaxial compression tests to measure the elastic modulus of silica aerogel, J. Non-Cryst. Solids 354 (2008) 4556–4561.
[15] T. Woignier, J. Pelous, J. Phalippou, R. Vacher, E. Courtens, Elastic properties of silica aerogels, J. Non-Cryst. Solids 95&96 (1987) 1197–1202.
[16] T. Woignier, J. Phalippou, Mechanical strength of silica aerogels, J. Non-Cryst. Solids 100 (1988) 404–408.
[17] R. Haj-Ali, R. Eliasi, V. Fourman, C. Tzur, G. Bar, E. Grossman, R. Verker, R. Gvishi,

I. Gouzman, N. Eliaz, Mechanical characterization of aerogel materials with digital image correlation, Micropor. Mesopor. Mat. 226 (2016) 44–52.
[18] T.E. Gomez Alvarez-Arenas, F.R. Montero De Espinosa, M. Moner-Girona, E. Rodriguez, A. Roig, E. Molins, Viscoelasticity of silica aerogels at ultrasonic frequencies, Appl. Phys. Lett. 81 (2002).
[19] J. Groby, T. Schlief, J. Fricke, Ultrasonic evaluation of elastic properties of silica aerogels, Mater. Sci. Eng. 168 (1993) 235–238.
[20] V. Romero-García, G. Theocharis, V. Pagneux, O. Richoux, Use of complex frequency plane to design broadband and sub-wavelength absorbers, J. Acoust. Soc. Am. 139 (2016) 3395–3403.
[21] K.F. Graff, Wave Motion in Elastic Solids, Dover Publications, New York, 1975.
[22] B.H. Song, J.S. Bolton, A transfer-matrix approach for estimating the characteristic impedance and wave numbers of limp and rigid porous materials, J. Acoust. Soc. Am. 107 (2000) 1131.
[23] M.R. Stinson, The propagation of plane sound waves in narrow and wide circular tubes, and generalization to uniform tubes of arbitrary crosssectional shape, J. Acoust. Soc. Am. 89 (1991) 550–558.
[24] M. Niskanen, J.-P. Groby, A. Duclos, O. Dazel, J.C. Le Roux, N. Poulain, T. Huttunen, T. Lahivaara, Deterministic and statistical characterization of rigid frame porous materials from impedance tube measurements, J. Acoust. Soc. Am. 142 (2017) 2407–2418.
[25] Y. Censor, Pareto optimality in multiobjective problems, Appl. Math. Optimiz. 4 (1977) 41–59.
[26] T. Back, Selective pressure in evolutionary algorithms: a characterization of selection mechanisms, Proceedings of the First IEEE Conference on Evolutionary Computation, IEEE Press, Orlando, 1994, pp. 57–62.
[27] L. Forest, V. Gibiat, T. Woignier, Biot's theory of acoustic propagation in porous media applied to aerogels and alcogels, J. Non-Cryst. Solids 225 (1998) 287.
[28] J. Gross, G. Reichenauer, J. Fricke, Mechanical properties of SiO_2 aerogels, J. Phys. D 21 (1988) 1447.
[29] N. Jiménez, W. Huang, V. Romero-García, V. Pagneux, J.-P. Groby, Ultra-thin metamaterial for perfect and quasi-omnidirectional sound absorption, Appl. Phys. Lett. 109 (2016) 121902.
[30] N. Jiménez, V. Romero-García, V. Pagneux, J.-P. Groby, Rainbow-trapping absorbers: broadband, perfect and asymmetric sound absorption by subwavelength panels for transmission problems, Sci. Rep. 7 (13595) (2017).